New Phytologist

Research

The roles of *AaMIXTA1* in regulating the initiation of glandular trichomes and cuticle biosynthesis in *Artemisia annua*

Pu Shi, Xueqing Fu, Qian Shen, Meng Liu, Qifang Pan, Yueli Tang, Weimin Jiang, Zongyou Lv, Tingxiang Yan, Yanan Ma, Minghui Chen, Xiaolong Hao, Pin Liu, Ling Li, Xiaofen Sun and Kexuan Tang

Key Laboratory of Urban Agriculture (South) Ministry of Agriculture, Plant Biotechnology Research Center, Fudan-SJTU-Nottingham Plant Biotechnology R&D Center, School of Agriculture and Biology, Shanghai Jiao Tong University, Shanghai 200240, China

Authors for correspondence:
Kexuan Tang
Tel: +86 2134206916
Email: kxtang@sjtu.edu.cn

Received: *8 March 2017*
Accepted: *14 August 2017*

New Phytologist (2017)
doi: 10.1111/nph.14789

Key words: AaMIXTA1, *Artemisia annua* L., artemisinin, epidermal cuticle, glandular secretory trichomes (GSTs).

Summary

- The glandular secretory trichomes (GSTs) on *Artemisia annua* leaves have the capacity to secrete and store artemisinin, a compound which is the most effective treatment for uncomplicated malaria. An effective strategy to improve artemisinin content is therefore to increase the density of GSTs in *A. annua*. However, the formation mechanism of GSTs remains poorly understood.
- To explore the mechanisms of GST initiation in *A. annua*, we screened myeloblastosis (MYB) transcription factor genes from a GST transcriptome database and identified a MIXTA transcription factor, AaMIXTA1, which is expressed predominantly in the basal cells of GST in *A. annua*. Overexpression and repression of *AaMIXTA1* resulted in an increase and decrease, respectively, in the number of GSTs as well as the artemisinin content in transgenic plants.
- Transcriptome analysis and cuticular lipid profiling showed that AaMIXTA1 is likely to be responsible for activating cuticle biosynthesis. In addition, dual-luciferase reporter assays further demonstrated that AaMIXTA1 could directly activate the expression of genes related to cuticle biosynthesis.
- Taken together, AaMIXTA1 regulated cuticle biosynthesis and prompted GST initiation without any abnormal impact on the morphological structure of the GSTs and so provides a new way to improve artemisinin content in this important medicinal plant.

Introduction

In plants, trichomes are small specialized organs derived from plant epidermal cells (Schilmiller *et al.*, 2008; Olsson *et al.*, 2009), and play important roles in resistance to biotic and abiotic stresses, such as herbivores, water absorption and UV radiation (Mauricio & Rausher, 1997; Serna & Martin, 2006). Two types of trichomes, namely glandular secretory trichomes (GSTs) and T-shaped nonsecretory trichomes (TSTs) occur in the traditional Chinese medicinal plant *Artemisia annua* and both are multicellular structures (Schilmiller *et al.*, 2008). A GST is a 10-celled biseriate elaborate structure with five cells on each side, containing two basal cells, two stalk cells, four subapical cells, and two apical cells (Duke & Paul, 1993; Olsson *et al.*, 2009). *Artemisia annua* trichomes are the site for the accumulation of various secondary metabolites, for example, numerous monoterpenes, sesquiterpenoids and related chemicals (Slone & Kelsey, 1985; Marco & Barbera, 1990). Especially, artemisinin, as the most pharmaceutical value component, is mainly produced and stored in GST (Duke & Paul, 1993; Olsson *et al.*, 2009).

Artemisinin is a sesquiterpene lactone with an endoperoxide bridge. Artemisinin-based combination therapies (ACTs) are considered as the most effective treatment for malaria recommended by World Health Organization (Mutabingwa, 2005; Graham *et al.*, 2010; Weathers *et al.*, 2011). Besides its antimalarial function, artemisinin has also been reported to have antiviral, anticancer and antischistosomal activities (Efferth, 2006; Romero *et al.*, 2006; Utzinger *et al.*, 2007), resulting in its high demand by the pharmaceutical industry. Unfortunately, the supply of artemisinin is significantly restricted by the low content of artemisinin (0.01–0.1% leaf DW) in *A. annua* (Abdin *et al.*, 2003). To date, numerous efforts have been made to elucidate the artemisinin biosynthetic pathway (Supporting Information Fig. S1; Tang *et al.*, 2014). Previous studies have demonstrated that the enzymes relating to the artemisinin biosynthetic pathway – amorpha-4,11-diene synthase (ADS), cytochrome P450-dependent hydroxylase (CYP71AV1), artemisinic aldehyde reductase (DBR2) and aldehyde dehydrogenase 1 (ALDH1) – were located in the GSTs of *A. annua* (Olsson *et al.*, 2009; Wang *et al.*, 2013). Thereby, GSTs play a crucial role in artemisinin biosynthesis. Manipulating GST initiation is the key to being able to improve the artemisinin content in *A. annua* without having to completely understand the biochemistry of artemisinin production.

In plants, myeloblastosis (MYB) proteins regulate trichome development, root hair density, secondary metabolism, and

response to biotic and abiotic stresses (Stracke *et al.*, 2007; Wester *et al.*, 2009; Khosla *et al.*, 2014; Matias-Hernandez *et al.*, 2017). MYB proteins constitute a large transcription factor family in plants and are divided into four subfamilies according to the number of imperfect MYB domain repeats (Dubos *et al.*, 2010; Feller *et al.*, 2011). The largest subfamily group of MYB transcription factors is the R2R3 MYBs, generally containing two imperfect MYB repeats near the N-terminus, and transcriptional activation or inhibition domains closer to the C-terminus (Martin & Paz-Ares, 1997). Furthermore, the R2R3MYB subfamily is divided into 22 subgroups based on the differences in their C-termini (Martin & Paz-Ares, 1997; Jungblut *et al.*, 1999; Dubos *et al.*, 2010). MIXTA or MIXTA-like transcription factors are subgroup9, many of which control cell shape, trichome development and seed fiber initiation in multiple plant species (Walford *et al.*, 2011; Brockington *et al.*, 2013; Oshima *et al.*, 2013). Among the identified transcription factors, AmMIXTA from *Antirrhinum majus* was the first characterized subgroup9 member to affect pigmentation and shape of petals conical epidermal cells (Noda *et al.*, 1994; Martin *et al.*, 2002). GhMYB25 and GhMYB25-like were two MIXTA type transcription factors and predominantly expressed in the ovule epidermis during fiber initiation in tetraploid *Gossypium hirsutum*, and thereby affected the initiation and timing of fiber initial expansion (Machado *et al.*, 2009; Walford *et al.*, 2011). Moreover, AtMYB106 and AtMYB16 regulated trichome branch formation and epidermal cell morphology in Arabidopsis (Oshima *et al.*, 2013). However, MYB transcription factors, especially the MIXTA subgroup involved in GST initiation, have not been reported in *A. annua*.

The cuticle layer is made up of polymerized cutin matrix and ubiquitous aliphatic waxes to provide the mechanical strength and viscoelasticity for the plants (Pollard *et al.*, 2008; Samuels *et al.*, 2008; Go *et al.*, 2014). The load and composition of cutin and cuticular waxes show remarkable differences between tissues and organs in plants (Bernard & Joubes, 2013; Go *et al.*, 2014). The *glassy hair 6* (*glh6*) mutant of Arabidopsis showed obvious variation in branching, size and glossiness of trichomes, and affected cuticular wax biosynthesis (Zheng *et al.*, 2005; Suo *et al.*, 2013). In *Arabidopsis thaliana*, *ATP-binding cassette G family member 11* (*abcg11*) mutants exhibited noticeable alterations of leaf surface cutin monomers. Scanning electron microscopy images demonstrated that the branching patterns and surface morphology of trichomes were abnormal in the *abcg11* mutant (Panikashvili *et al.*, 2007). Therefore, these results implied that there was a relationship between trichome development and cuticle biosynthesis. In particular, some MIXTA transcription factors regulating cuticle biosynthesis are also involved in trichome development. AtMYB106 and AtMYB16 controlled the epidermal cell morphology and cuticle accumulation through the independent regulation of wax biosynthesis in *A. thaliana* (Oshima *et al.*, 2013). In addition, AtMYB106 participated in the regulation of cuticle biosynthesis by coordinating with an APETALA2/ETHYLENE RESPONSE FACTOR (AP2/ERF), WAXES INDUCER1/SHINE1 (WIN1/SHINE1; Kannangara *et al.*, 2007; Oshima *et al.*, 2013). However, the relationship between trichome formation and components of cutin and cuticular waxes remains unclear.

In the present study, we isolated and characterized the *AaMIXTA1* gene from the glandular trichome transcriptome database of *A. annua*. *AaMIXTA1* encodes an R2R3MYB transcription factor, which upregulates the number of GST on leaves. We also analyzed the content of cuticular waxes and cutin monomers in *AaMIXTA1* knockdown and *AaMIXTA1* overexpressing transgenic plants, respectively. The results demonstrated that AaMIXTA1 was a positive regulator of cuticular wax and cutin biosynthesis, as well as a critical regulator of glandular trichome formation in *A. annua*.

Materials and Methods

Plant materials and growth conditions

Plants from the widely grown *Artemisia annua* L. cultivar, called Huhao 1, have been selected and developed over several years at our university (Shen *et al.*, 2016). They were grown under 16 h : 8 h, light : dark photoperiod at 25 ± 2°C. *Nicotiana benthamiana* grown at 25 ± 2°C under a 16 h light photoperiod was used in transient transformation.

Phylogenetic tree and global expression of MYB family

Artemisia annua myeloblastosis (MYB) transcription factors were identified from our unpublished transcriptome of laser-captured glandular secretory trichome (GST) cells using BLASTP queries with the known *Arabidopsis* MYBs. The RNA-seq data (SRR019547 for mature leaf trichome; SRR019254 for meristem; SRR019548 for bud trichome; SRR019549 for cotyledon; SRR019546 for young leaf trichome) were obtained from the National Center for Biotechnology Information (NCBI) Sequence Read Archive (SRA) database (Graham *et al.*, 2010). The data were converted to fasta format using the SRA toolkit (http://www.ncbi.nlm.nih.gov/Traces/sra/?view=software). The reads of MYB transcription factors in cotyledon, mature leaf trichome, meristem, flower bud trichome and young leaf trichome were obtained by BLASTN search against the glandular trichome transcriptome database with $E < 10^{-6}$. The read counts were normalized by reads per kilobase per million mapped reads (RPKM) for each transcript in different tissue samples. Hierarchical cluster analysis was performed using a MultiExperiment Viewer (MeV, v.4.9.0; Zhang *et al.*, 2015). The putative MYB transcription factor sequences of *A. annua* and *A. thaliana* were aligned by ClustalX (Trinity College, Dublin, Ireland). The phylogenetic tree was constructed by Mega5 software (Tamura *et al.*, 2011). Protein sequences of MIXTA or MIXTA-like transcription factors (TFs) from other species were also gathered using the NCBI. To obtain the open reading frame (ORF) of *AaMIXTA1*, cDNA was synthesized with 0.5 μg of total RNA isolated from leaves of *A. annua*, and the ORF was amplified using the gene-specific primers in Table S1.

Quantitative real-time PCR

For gene expression analyses, total RNA samples were isolated from different tissues and leaves from different phyllotaxis of *A. annua* by using RNAprep pure Plant Kit (Tiangen Biotech, Beijing, China) following the manufacturer's instruction. Different tissues (flower bud, young leaf, flower, stem and root) of the wild-type plants were collected from 6-month-old *A. annua* grown in the field. Moreover, the leaves leaf0 (including meristem), 1, 2, 3, 4, 5, 7, 9 and 15 counted from the apical top of the main stem were collected from 5-month-old *A. annua*. The RNA samples were reverse-transcribed into cDNA using the PrimeScript II 1st Strand cDNA Synthesis Kit (Takara, Dalian, China) following the manufacturer's instruction. Quantitative RT-PCR analysis was carried out with the cDNA using SYBR green on a Roche LightCycler 96 real-time PCR machine (Roche, Basel, Switzerland). The β-*Actin* was used as reference gene for standardization of the results. The relative expression levels were calculated as described previously (Livak & Schmittgen, 2001). Three biological repeats were measured for each sample. The primers used were shown in Table S2.

Subcellular localization of AaMIXTA1

The full-length of *AaMIXTA1* without the termination codon was cloned into the pENTR-D-TOPO vector (Invitrogen), and subsequently recombined into the destination vector pEarleyGate105 (YFP protein in pEarleygate 101 was replaced by mcherry and the vector was named as pEarleyGate 105) by Gateway LR recombination reaction (Invitrogen). The recombinant plasmid was introduced into *Agrobacterium tumefaciens* strain GV3101 for *N. benthamiana* leaf transient expression (Sparkes *et al.*, 2006). The fluorescent signals were observed under a laser confocal scanning microscope Leica TCS SP5 (Leica Microsystems, Wetzlar, Germany).

Molecular cloning of *AaMIXTA1* promoter and promoter-GUS fusion in transgenic *A. annua*

Genomic DNA was extracted from fresh young leaves of *A. annua*. The upstream 2596 bp of *AaMIXTA1* was obtained from the genome database of *A. annua* (unpublished results), amplified using PCR containing *Pst*I and *Bam*HI restriction sites and inserted into pCAMBIA1391Z vector. After confirmation by sequencing, the recombinant plasmid was transformed into *A. tumefaciens* strain EHA105. The positive clone was identified by PCR and used for plant transformation (Zhang *et al.*, 2009). The different tissues were sampled from primary transformants for histochemical β-glucuronidase (GUS) staining (Jefferson *et al.*, 1987). The stained tissues were rinsed with 75% ethanol solution at 60°C to completely remove chlorophyll. Observations were performed using a light microscope OLYMPUS BX51 (Olympus, Tokyo, Japan). The AaMIXTA1 promoter was amplified using the primers in Table S1.

Construction and transformation of *A. annua*

The 1137-bp full-length AaMIXTA1 was amplified with *Bam*HI and *Pst*I restriction sites from a cDNA pool using KOD DNA polymerase (Toyobo, Osaka, Japan) following the manufacturer's protocol. The fragment was digested with *Bam*HI and *Pst*I, and subsequently cloned into the pHB eventual binary vector. An ethylene response factor-associated amphiphilic repression (EAR) domain was introduced into the downstream of *AaMIXTA1* containing *Bam*HI and *Pst*I restriction sites using specific primers. The *AaMIXTA1-EAR* fragment was cloned into the pHB eventual binary vector. The 300-bp nonconservative *AaMIXTA1* fragment was amplified, cloned into gateway cloning vector pENTR vector using pENTR™/SD/D-TOPO® Cloning Kit (Invitrogen) and then transferred to the destination vector pHELLSGATE12 (Karimi *et al.*, 2007) via the LR recombination reaction (Invitrogen). The recombination plasmids (pHB-AaMIXTA1, pHELLSGATE12-AaMIXTA1-RNAi and AaMIXTA1-EAR) and empty vector plasmids (pHB and pHELLSGATE12) were introduced into *A. tumefaciens* strain EHA105 and transformed into *A. annua* plants, as described previously (Zhang *et al.*, 2009). All analyses were done on the primary transformants and overexpression and silencing lines compared to plants transformed with empty vectors as controls. The primers used are listed in Table S1.

GST density counting

The mature and expanded leaves (leaf6, the sixth leaf below apical meristem) were collected from plants grown under the same conditions. GSTs on the leaf adaxial sides in transgenic *A. annua* and control were observed for quantification of GST density. The number of trichomes represents the total number of trichomes within a 1-mm^2 area of the leaf. The number of GSTs were counted from micrographs using ImageJ software (http://rsb.info.nih.gov/ij) reported previously (Cheng *et al.*, 2014). Leaf samples were collected from three different independent transformants. For each independent plant, we selected three different leaves at the same position for counting.

Scanning electron microscopy

Tissues were collected and processed using a standard protocol for scanning electron microscopy (SEM; Chuartzman *et al.*, 2008). To observe the structure of the cuticle and trichomes, the sixth leaf counted from the apical meristem *OE-AaMIXTA1*, *AaMIXTA1-EAR* and empty vector (pHB) *A. annua* were fixed in 0.1 M phosphate buffer containing 2.5% glutaraldehyde (pH 7.4), at 4°C for 12 h. Samples were rinsed 4 times in 0.1 M phosphate buffer (pH 7.4) for 15 min each time, dehydrated for 30 min through a series of alcohol (50%, 60%, 70%, 80%, 95% and 100%) and dried in a critical point drying device (Leica EM CPD030). The samples were coated with 20 Å gold particles, and observations were made by SEM (Nova NanoSEM 230; FEI Company, Hillsboro, OR, USA; Go *et al.*, 2014).

Cuticle analysis of *A. annua* leaves using gas chromatography mass spectrometry

For wax analyses, fresh leaves from transgenic lines were powdered in liquid nitrogen and dried in a vacuum freeze dryer for 3 d. We weighed 0.1 g powder and immersed it in chloroform (5 ml) for ultrasonication. The supernatant was filtered through a 0.25 μm-pore-size filter. The solvents were removed with a gentle stream of nitrogen gas and then redissolved in a mixture of 20 μl of pyridine (Sigma) and 20 μl of bis-*N*, *N*-(trimethylsilyl) trifluoroacetamide (BSTFA; Sigma). The mixture was incubated for 1 h at 70°C for derivatization. Metabolite analysis was performed using a Gas Chromatograph-Mass Spectrometer (7890A-5975C; Agilent Technologies Inc., Santa Clara, CA, USA). An HP-5MS capillary column (30 m, 0.25 mm, 0.25 μm) was used to separate components. The injection temperature was set at 250°C. Pure helium was used as the carrier gas, with a flow rate of 1 ml min^{-1}. All ingredient peaks within samples were recorded and stored as Agilent Data files (Lee & Suh, 2015). For cutin deposition analysis, the polyesters were depolymerized by boron trifluoride in methanol (BF3/MeOH) for cleaving ester bounds, and released solvent extractable methyl esters suitable for chromatography mass spectrometry (GC-MS) analysis (Franke *et al.*, 2005). Each leaf sample was collected from three individual plants in the same growth conditions.

Dual-luciferase (dual-LUC) transient assay

The promoters of *3-ketoacyl-CoA synthase 5* (*AaKCS5*), *3-ketoacyl-CoA synthase 1* (*AaCER1*), *cytochrome P450 77A1* (*AaCYP77A1*), *cytochrome P450 86A1* (*AaCYP86A1*) and *ATP-binding cassette G12* (*AaABCG12*) were cloned based on the *A. annua* genome database (unpublished results), and (respectively) inserted into pGreenII0800-LUC vector. The recombinant plasmid was introduced into *A. tumefaciens* strain GV3101 with the plasmid pSoup19 as the reporters. For dual-LUC assay, pHB-AaMIXTA1 plasmid was transformed into GV3101 to act as effector for *A. tumefasciens*-based *N. benthamiana* leaf transient expression (Voinnet *et al.*, 2003). The pHB empty construct was used as negative control. The method has been reported previously (Liu *et al.*, 2008). Luciferase activities were measured using the Dual-Luciferase® Reporter Assay System (Promega; Hellens *et al.*, 2005). Each sample was collected from three individual plants in the same growth conditions.

Quantification of artemisinin using HPLC-ELSD

Artemisia annua leaves were collected at the same growth period and dried at 50°C for 48 h. Three biological repeats were measured for each sample. The artemisinin content was analyzed using a Waters Alliance 2695 high-performance liquid chromatography (HPLC) system coupled with a Waters 2420 evaporative light scattering detection (ELSD) tool as described previously (Zhang *et al.*, 2009).

RNA-seq analysis

The total RNA samples were isolated from the meristem and small leaf primordia of *AaMIXTA-RNAi-3* transgenic line and empty vector control plant by using RNAprep pure Plant Kit (Tiangen Biotech) following the manufacturer's instruction. The quality control was performed using an Agilent 2100 Bioanalyzer (Agilent Technologies Inc.). To analyze the transcriptome, RNASeq libraries were prepared from cDNA by Majorbio (Shanghai, China) and sequenced on an Illumina Hiseq4000 (Illumina Inc., San Diego, CA, USA). Raw sequencing reads were screened with the SeqPrep software (https://github.com/jstjohn/SeqPrep) and Sickle software (https://github.com/najoshi/sickle) to cut out low quality or default reads. All gained reads were assembled to contigs and singletons. The ORF prediction was carried out using the novel method Trinity (http://trinityrnaseq.sourceforge.net/). Gene expression (FPKM) and differential expression levels were analyzed using Rsem (http://deweylab.biostat.wisc.edu/rsem/) and edgeR software (http://www.bioconductor.org/packages/2.12/bioc/html/edgeR.html). We defined gene function annotation from the assembled ORFs using Blastx with the NCBI-NR (nonredundant) database, String, Swissprot and the Kyoto encyclopedia of genes and genomes (KEGG).

Accession numbers

Sequence data in this article were deposited in the GenBank databases under the following accession numbers: *AaMIXTA1* (KP195023), *AaCYP77A1* (MF197860), *AaCYP86A1* (MF197861), *AaKCS5* (MF197858), *AaCER1* (MF197859), *AaABCG12* (MF197862), *proAaMIXTA1* (MF144187), *proAaCYP77A1* (MF144189), *proAaCYP86A1* (MF144190), *proAaKCS5* (MF144188), *proAaCER1* (MF144191) and *proAaABCG12* (MF144192).

Cytochrome P450 sequence data for this article can be found in the following website: http://drnelson.uthsc.edu/cytochromeP450.html. Official P450 numbers: *AaCYP77A1* (CYP77B35 *A. annua*), *AaCYP86A1* (CYP86A150 *A. annua*).

Raw RNA-seq data are available from the NCBI Sequence Read Archive (SRA; accession number: SRR5714147).

Results

Identification and characterization of AaMIXTA1 involved in the plant tissue development

First, we isolated *A. annua* GST using laser capture microdissection (LCM) methodologies published previously (Matas *et al.*, 2011; Olofsson *et al.*, 2012) and extracted GST RNA for performing RNA-seq. We screened the GST transcriptome database (P. Shi *et al.*, unpublished data) and identified 97 MYB proteins by performing a Blastp analysis with *Arabidopsis* MYB proteins (Fig. 1a). All 97 MYBs' expression levels were analyzed based on other published databases (Graham *et al.*, 2010) from different *A. annua* tissues to look for which of those MYBs (nine genes) that were coexpressed with the known enzymes for artemisinin biosynthesis (Fig. 1a). Furthermore, several MYB transcription

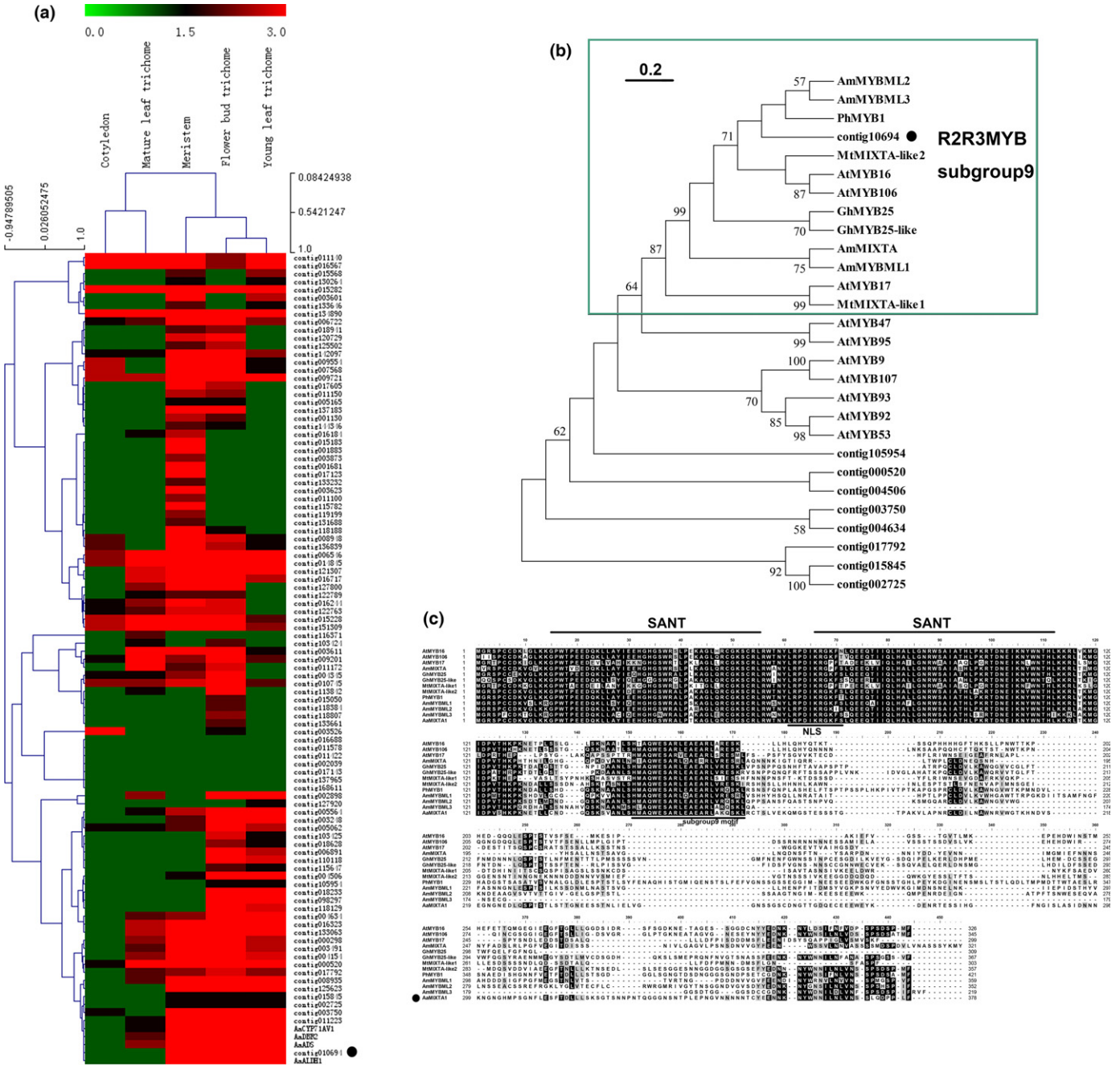

Fig. 1 Identification and characterization of *AaMIXTA1*. (a) Hierarchical cluster analysis of myeloblastosis (MYB) transcription factors in glandular secretory trichomes (GSTs) of *Artemisia annua*. The color scale at the top represents the value of log-transformed reads per kilobase per million mapped reads. (b) Phylogenetic tree showing the relationship of MYB transcription factors predominantly expressed in young leaf trichomes, flower bud trichomes and shoot tips of *A. annua* compared with MYB transcription factors involved in organ development and cell differentiation. The previously described subgroup9 containing MIXTA/MIXTA-like MYBs are highlighted by in green. *Gossypium hirsutum* (Gh), *Antirrhinum majus* (Am), *Petunia hybrida* (Ph), *Medicago truncatula* (Mt), *Arabidopsis* (At). (c) Alignment of the deduced protein sequences of AaMIXTA1 and MIXTA/MIXTA-like proteins from other species. The sequences were aligned by BIOEDITOR software (University of California, San Diego, CA, USA). The MYB domain and motif characteristic of subgroup9 are represented by a line above the sequence. The putative nuclear localization signal (NLS) is highlighted by a line below the protein sequence. The candidate gene is indicated by the black dots.

factors are reported to be involved in the initiation and development of trichomes in other plant species, especially MIXTA and MIXTA-like genes belonging to subgroup9 (Brockington *et al.*, 2013). Phylogenetic analysis of our nine identified candidate MYBs showed that only one, contig10694, clustered with the MIXTA-like transcription factors AtMYB16 and AtMYB106 that have a known function in trichome initiation and development in Arabidopsis (Oshima *et al.*, 2013; Fig. S2). Further analysis indicated that contig10694 also clustered with the MIXTA factors from other species (Fig. 1b). Therefore, contig10694,

designated AaMIXTA1, was selected as a candidate gene for further investigation. An amino acid alignment was performed against all of the proteins clustering with AaMIXTA1. High sequence conservation was noted at the N-terminus within the two MYB repeat domains known to be important for DNA binding. The presence of signature domain 'HMAQWESARLEAEARLxRxS' demonstrated that AaMIXTA1 belonged to the subgroup9 of R2R3MYB factors (Stracke *et al.*, 2001; Brockington *et al.*, 2013; Fig. 1c). In addition, a putative monopartite nuclear localization signal (NLS), LRPDIKRGKFS, was predicted between the two MYB repeats of AaMIXTA1 by the NLS mapper website (http://nls-mapper.iab.ke io.ac.jp/cgi-bin/NLS_Mapper_form.cgi; Fig. 1c).

AaMIXTA1 is localized in the nuclei and expressed predominantly in the basal cells of GST in *A. annua*

In order to further investigate the subcellular localization of AaMIXTA1, mCherry was fused to the C-terminus of AaMIXTA1. As shown in Fig. 2(a), mCherry fluorescent was observed in the nucleus of *N. benthamiana* epidermal cells, demonstrating that AaMIXTA1 was localized in the nucleus. The expression of AaMIXTA1 in different tissues of *A. annua* was examined by quantitative RT-PCR. The results showed that *AaMIXTA1* was expressed in stem, young leaf, flower bud and mature flowers, with highest expression in flower buds (Fig. 2b). *AaMIXTA1* expression was higher in the youngest leaf (leaf0) than other leaves and rapidly decreased with leaf age (Fig. 2c). To further examine *AaMIXTA1*'s tissue-specific expression pattern, we cloned a 2569-bp promotor sequence of *AaMIXTA1* based on sequences from our genome database (unpublished data). This fragment was introduced upstream of *GUS* coding region and transformed into *A. annua* using *Agrobacterium*-mediated method. GUS staining showed that *AaMIXTA1* was highly expressed in the shoot tip (Fig. 2d,f) of *A. annua*, as well as in the youngest leaf (Fig. 2e). GUS staining was stronger in glandular trichomes than in other regions (Fig. 2g), and restricted primarily to the two basal cells of glandular trichomes (Fig. 2h). GUS activity in the apical meristem was further studied by light microscopy using epoxy semi-thin sections. GUS activity was clearly observed in the two basal cells of the 10-celled biseriate elaborate glandular trichomes of the apical meristem (Fig. 2i). These results indicated that *AaMIXTA1* is predominantly expressed in the basal cells of *A. annua* GST.

AaMIXTA1 is a positive transcription factor regulating GST initiation in *A. annua*

In order to further explore the function of AaMIXTA1 in *A. annua*, we generated transgenic *A. annua* overexpressing *AaMIXTA1* driven by cauliflower mosaic virus (CaMV) 35S promoter. Quantitative RT-PCR analysis revealed that *AaMIXTA1* expression was significantly increased in transgenic lines (Fig. 3h). The GST numbers on the leaf adaxial side in three independent *OE-AaMIXTA1* lines increased 1.3- to 1.5-fold compared with those of the empty vector control (Fig. 3a,b,e). SEM was used to investigate any changes in the GSTs and TSTs on the adaxial sides of mature leaves. All three transgenic lines examined had an obvious increase in GST numbers compared with that of the control and correlated with the increase in *AaMIXTA1* transcript levels (Fig. 4a,b). In addition, the artemisinin content in the *OE-AaMIXTA1* lines was increased from *c.* 8 to 16 mg g^{-1} DW compared to the control (Fig. 4j). On the contrary, suppressing *AaMIXTA1* expression using RNAi under the CaMV 35S promoter produced lines with a 41–53% decrease in *AaMIXTA1* transcripts (Fig. 3i). Densities of GSTs in these *AaMIXTA1-RNAi* lines were found to have been decreased by 26–33% (Fig 3a,c,f). Likewise, the artemisinin contents was decreased to 6–6.51 mg g^{-1} DW in *AaMIXTA1-RNAi* lines (Fig. 4k). To further analyze the function of AaMIXTA1, *AaMIXTA1-EAR* plants expressing a chimeric repressor were generated. *AaMIXTA1* expression was increased in *AaMIXTA1-EAR* transgenic plants (Fig. 3j). A detailed observation of GSTs revealed that the repression of AaMIXTA1 downstream target genes significantly reduced GST densities on the adaxial sides of mature leaves in transgenic *A. annua* (Fig. 3d,g). These results were further confirmed by SEM observation (Fig 4a,c). The artemisinin content was also decreased to 4.69–5.61 mg g^{-1} DW relative to the empty vector controls that produced only 8.15 mg g^{-1} DW (Fig 4l). On the adaxial surface of mature leaves, no effect was observed on the morphology of the mature 10-celled GST structures in either the *OE-AaMIXTA1* or *AaMIXTA1-EAR* transgenic lines examined at the same developmental stages (Fig. 4d–f). Moreover, the phenotypes of TST with two filamentous structures on the base cells in both *OE-AaMIXTA1* and *AaMIXTA1-EAR* lines were also normal (Fig. 4a,g–i). Moreover, AaMIXTA1 positively regulated the TST number on the adaxial surface of mature leaves (Fig. S3). The densities of TST in *OE-AaMIXTA1* lines were increased by 25–32%, and those in *AaMIXTA1-RNAi* transgenic plants were decreased by 29–35% compared with the control. In *AaMIXTA1-EAR* lines (Fig. S3a,b), the density of line 6 was even reduced by 50% (Fig. S3a,c). These results demonstrate that AaMIXTA1 is a positive regulator of both GST and TST initiation in *A. annua.*

AaMIXTA1 positively affects cuticle deposition in *A. annua*

Accumulation of waxes and cutin monomers by GC-MS in the leaves of *OE-AaMIXTA1* and *AaMIXTA1-RNAi* transgenic lines was determined and compared to that of the empty vector control lines. Total wax in the *OE-AaMIXTA1* leaves increased by 10–40-%, and particularly the major cuticular waxes, including docosanoic acid, hexacosanoic acid, hexacosanol and β-amyrin (Fig. 5a). Moreover, the total cutin monomer load on the surface of mature leaves in *OE-AaMIXTA1* lines increased by 20–25% (Fig. 5b). The contents of 10, 16-diOH-Hexadecanoic, 16-OH-Hexadecanoic and monofunctional hexadecanoic acid increased significantly in *OE-AaMIXTA1* lines (Fig. 5b). By contrast, the accumulation of total waxes and cutin monomers decreased significantly in *AaMIXTA1-RNAi* lines (Fig. 5c,d). The total waxes in *AaMIXTA1-RNAi* leaves reduced by *c.* 50–77% (Fig. 5c). The concentrations of wax components, including docosanoic acid, hexacosanoic acid, dotriacontane, hexacosanol, octacosanol and

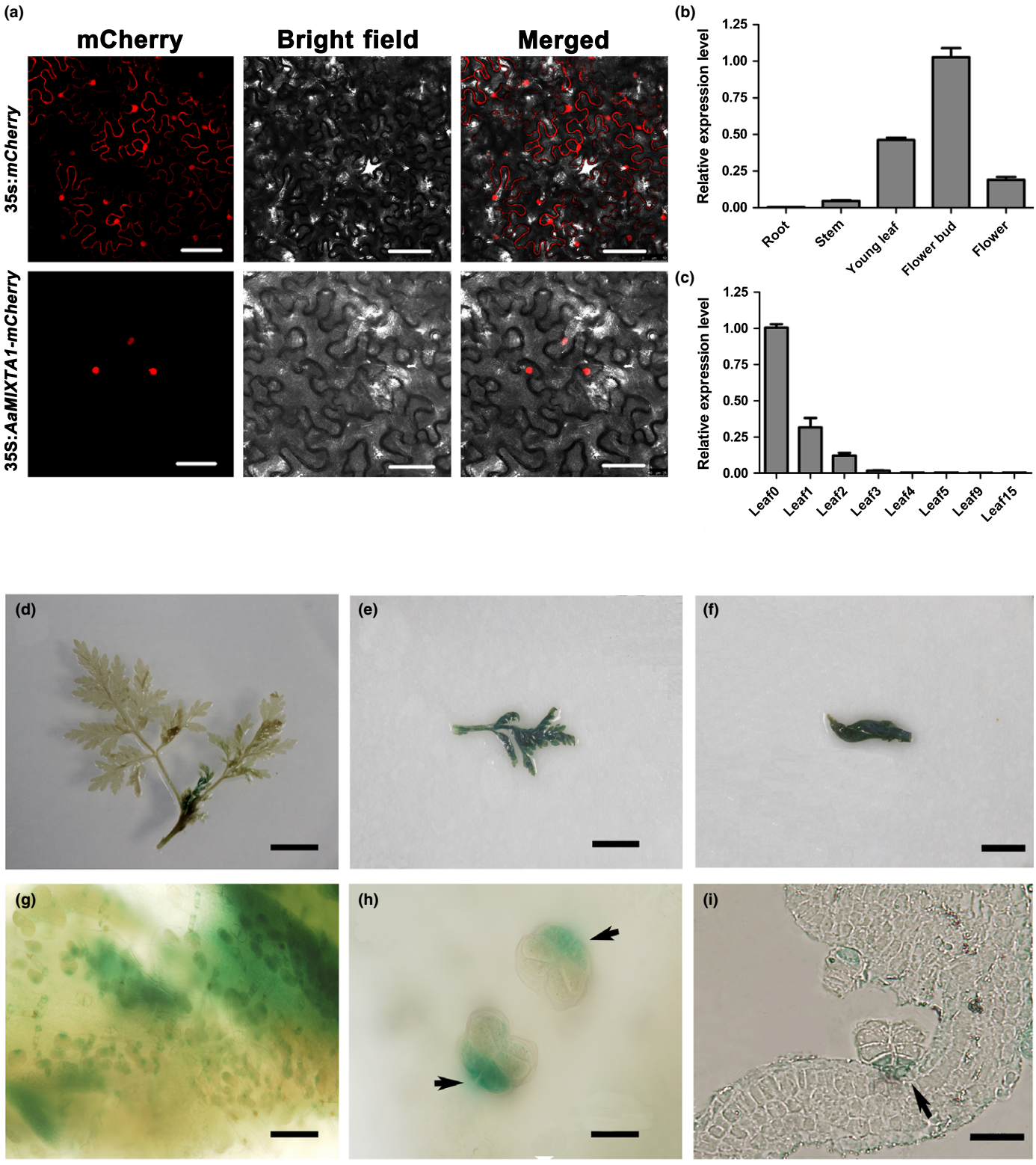

Fig. 2 *AaMIXTA1* is predominantly expressed in the basal cells of glandular secretory trichomes (GSTs) in *Artemisia annua*. (a) Subcellular localization of the AaMIXTA1 protein in *Nicotiana benthamiana* leaves. The fluorescence and bright field images collected by confocal microscopy are shown. (b) Relative expression of *AaMIXTA1* in root, stem, young leaf, flower bud and flower of *A. annua* by quantitative real-time polymerase chain reaction, respectively. (c) Relative expression of *AaMIXTA1* in *A. annua* leaves of different developmental ages. β-*Actin* was used as internal control. Three biological repeats are measured for each sample. Three technical replicates were used for each biological repeat. Data are given as means ± SD ($n = 3$). (d) Tissue-specific expression of *AaMIXTA1* promoter-GUS. (e) β-glucuronidase (GUS)-staining is observed in the youngest leaf, (f) in the shoot tip, (g) in GSTs of young leaf, (h) in the base cells of GST in young leaf and (i) in two basal cells of GST by light microscopy using epoxy resin-embedded thin sections. The GUS staining is indicated by black arrowheads. Bars: (a) 40 μm; (d) 2 cm; (e) 0.5 cm; (f) 0.2 cm; (g) 100 μm; (h, i) 20 μm.

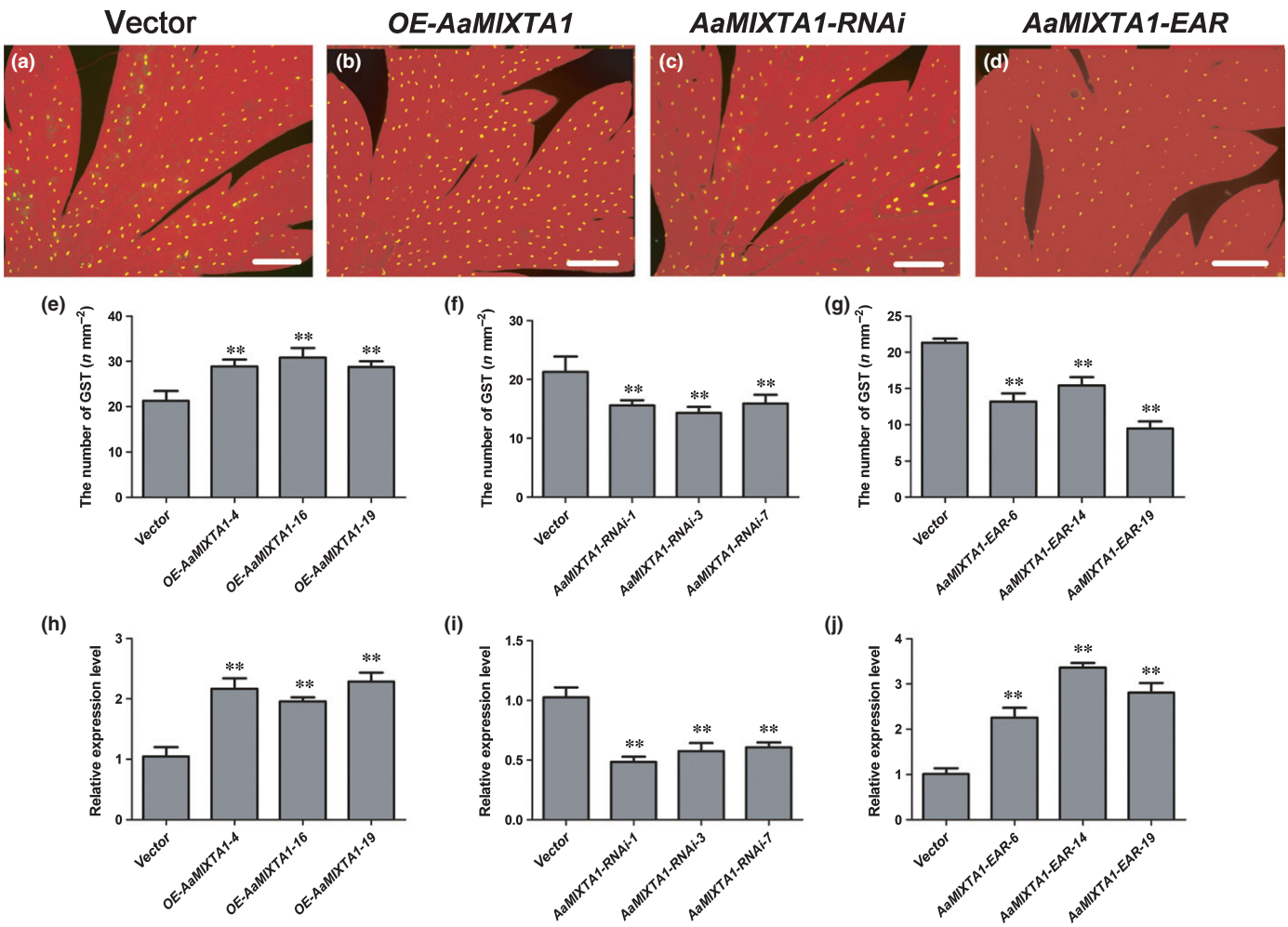

Fig. 3 The expression of *AaMIXTA1* regulates the glandular secretory trichomes (GSTs) initiation in *Artemisia annua*. (a) GST on the adaxial sides of mature leaves derived from empty vector (vector), (b) *OE-AaMIXTA1* transgenic *A. annua* plants, (c) *AaMIXTA1-RNAi* transgenic *A. annua* plants and (d) *AaMIXTA1-EAR* transgenic *A. annua* plants. The images were observed using fluorescence microscopy. Yellow spots represent GSTs. Red backgrounds represent chlorophyll. Bars: 0.8 mm. (e) The number of GSTs on the adaxial surface of leaves derived from empty vector (pHB) and *OE-AaMIXTA1* transgenic *A. annua* plants, (f) empty vector (pHELLSGATE12) and *AaMIXTA1-RNAi* transgenic *A. annua* plants, and (g) empty vector (pHB) and *AaMIXTA1-EAR* transgenic *A. annua* plants. A technical replicate was used for each biological repeat. Three biological repeats were measured for each sample. Data are given as means ± SD ($n = 3$). The numbers represent the total number of trichomes within a 1 mm^2 area of the leaf (e–g). (h) Expression level of *AaMIXTA1* in the *A. annua* leaves in *OE-AaMIXTA1* transgenic *A. annua* plants, (i) *AaMIXTA1-RNAi* transgenic *A. annua* plants and (j) *AaMIXTA1-EAR* transgenic *A. annua* plants. β-*Actin* was used as internal control for quantitative real-time polymerase chain reaction analysis. Three technical replicates were used for each biological repeat. Three biological repeats were measured for each sample. Data are given as means ± SD ($n = 3$). Asterisks indicate significant differences of the amounts between transgenic plants and the control by Student's *t*-test. **, $P < 0.01$.

β-amyrin, exhibited an obvious decrease in all three independent transgenic lines (Fig. 5c). The contents of 10, 16-diOH-Hexadecanoic, 16-OH-Hexadecanoic, hexadecanoic acid and octadecanoic acid were reduced in *AaMIXTA-RNAi* lines. However, the content of the major components of the waxes and cutin monomers, 9, 10, 18-triOH-Octadecanoic, were unchanged (Fig. 5b,d). This indicates that AaMIXTA1 regulates cuticle biosynthesis in *A. annua*.

AaMIXTA1 regulates the expression of genes related to cuticle biosynthesis in *A. annua*

RNA-seq experiments were carried out on *AaMIXTA1-RNAi-3* and empty vector control transgenic plants to better understand the impact of AaMIXTA1 on cuticle biosynthesis in *A. annua*. A total of 101 093 436 and 127 553 226 successful sequencing reads were produced for *AaMIXTA1-RNAi-3* and control lines, of which GC% was 43.97% and 43.84%, respectively (Table S3). Furthermore, 2583 differentially expressed genes between *AaMIXTA1-RNAi* and control plants were identified with a false discovery rate (FDR) < 0.05 and $\log_2|FC| \geq 1$ (Table S4). In the present study, we focused on the genes involved in the cuticle biosynthesis (Table 1). We identified 37 cuticle biosynthesis related genes, including the genes involved in epicuticular and intracuticular wax biosynthesis, polymerized cutin matrix biosynthesis and wax transport (Fig. 6a). Repression of *AaMIXTA1* transcript levels decreased the expression of 16 genes involved in the cuticle biosynthesis, including *AaCER1*, *AaWSD1*, *AaPAS2*, *AaCER2*, *AaCER6-like*, *AaCYP77A1*, *AaCYP86A1* and *AaABCG12* (Fig. 6a). In addition,

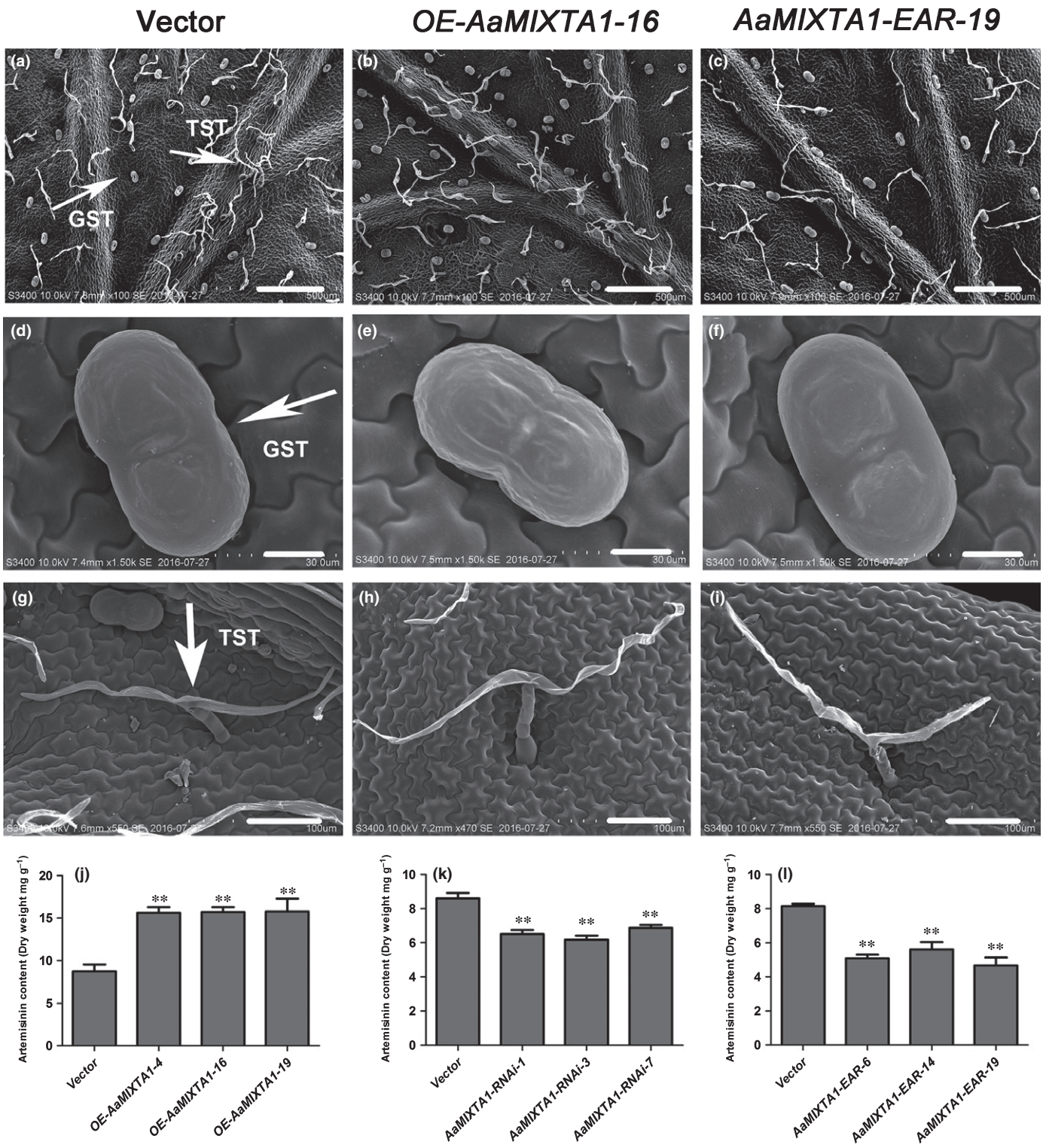

Fig. 4 Scanning electron microscope (SEM) analysis of the surface of leaves and high performance liquid chromatography (HPLC) analysis of the artemisinin content in transgenic *Artemisia annua* plants. (a–c) The glandular secretory trichome (GST) density was changed with the altered *AaMIXTA1* expression in transgenic *A. annua* plants. (a) GSTs and T-shaped nonsecretory trichomes (TSTs) on the adaxial sides of mature leaves derived from empty vector (pHB), (b) *OE-AaMIXTA1* transgenic *A. annua* plants and (c) *AaMIXTA1-EAR* transgenic *A. annua* plants. (d) The morphologies of GST on the leaf in empty vector (pHB), (e) *OE-AaMIXTA1* transgenic *A. annua* plants and (f) *AaMIXTA1-EAR* transgenic *A. annua* plants. (g) The morphologies of TST on the leaf in empty vector (pHB), (h) *OE-AaMIXTA1* transgenic *A. annua* plants and (i) *AaMIXTA1-EAR* transgenic *A. annua* plants. Bars: (a–c) 250 μm; (d–f) 15 μm; (g–i) 50 μm. The GST and TST are indicated by the white arrowheads. (j) The artemisinin contents (mg g^{-1} leaf DW) in transgenic *A. annua* plants of *OE-AaMIXTA1*, (k) *AaMIXTA1-RNAi* and (l) *AaMIXTA1-EAR*. Data are given as means ± SD ($n = 3$). Asterisks indicate significant differences of the amounts between transgenic *A. annua* plants and the control by Student's *t*-test. **, $P < 0.01$.

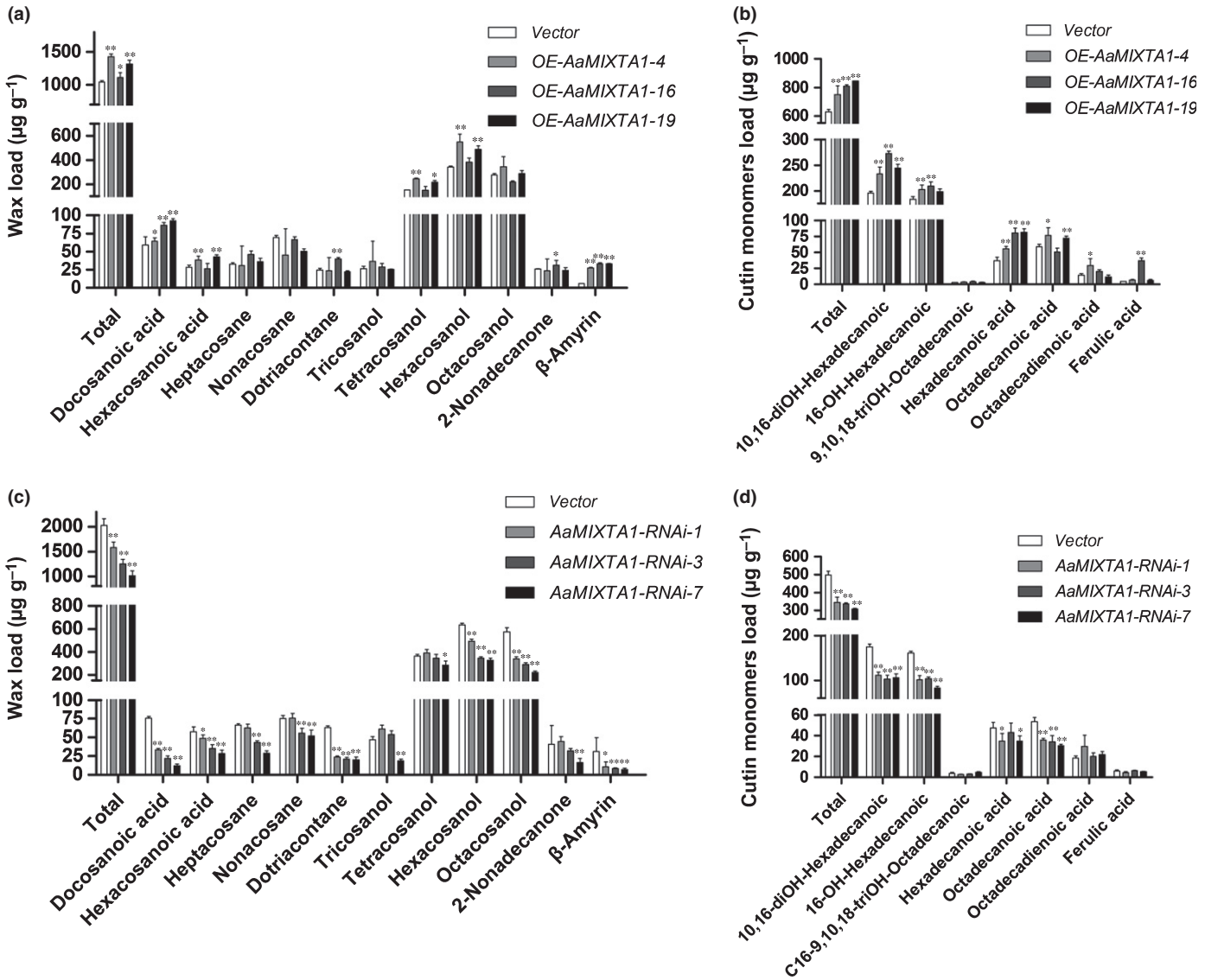

Fig. 5 Cuticle load analysis in empty vector (vector), *OE-AaMIXTA1* and *AaMIXTA1-RNAi* transgenic *Artemisia annua* plants. (a) Quantitative analysis of cutin and (b) waxes components in empty vector (pHB) and *OE-AaMIXTA1* transgenic *A. annua* plants. (c,d) Quantitative analysis of (c) cutin and (d) wax components in empty vector (pHELLSGATE12) and *AaMIXTA1-RNAi* transgenic *A. annua* plants. A technical replicate was used for each biological repeat. Three biological repeats are measured for each sample. Data are given as means ± SD ($n = 3$). Asterisks indicate significant differences of the amounts between transgenic *A. annua* plants and the control by Student's *t*-test. *, $P < 0.05$; **, $P < 0.01$.

the expression levels of *AaADS*, *AaDBR2* and *AaDXS* related to artemisinin biosynthesis were also reduced in *AaMIXTA1-RNAi* plants (Fig. 6b). Quantitative RT-PCR was performed to further verify AaMIXTA1 regulation on cuticle biosynthesis in multiple transgenic lines. The expressions of cutin- and wax-related synthase genes *AaCYP77A1*, *AaCYP86A1*, *AaABCG12*, *AaKCS5* and *AaCER1* were confirmed to be significantly reduced in both the *AaMIXTA1-RNAi-3* and *AaMIXTA1-RNAi-7* lines (Fig. 6c). The expressions of *AaADS*, *AaDBR2* and *AaDXS* were also reduced significantly in *AaMIXTA1-RNAi-3* transgenic lines (Fig. S4). The results of dual-LUC assay in *N. benthamiana* demonstrated that AaMIXTA1 significantly activated the expression of *AaKCS5*, *AaCER1*, *AaCYP77A1*, *AaCYP86A1* and *AaABCG12* (Fig. 6d). In conclusion, the results demonstrate that AaMIXTA1 upregulates cuticle biosynthesis in *A. annua*.

Discussion

AaMIXTA1 plays a positive role in the initiation of GST

AmMIXTA was the first subgroup9 myeloblastosis (MYB) to be reported and is a key regulator for the development of conical shaped petal epidermal cells (Noda *et al.*, 1994; Glover *et al.*, 1998). Subsequently, MIXTA or MIXTA-Like ortholog genes were reported as positive regulators in trichome development and epidermal cell differentiation. Overexpression of snapdragon *MYBML1* resulted in the abnormal differentiation of trichomes on carpels (Perez-Rodriguez *et al.*, 2005). Arabidopsis *myb106* mutant exhibited over-branched trichomes (Jakoby *et al.*, 2008). MIXTA-like R2R3 MYB (GUIDELESS) controls the formation of brushy hairs (trichomes) formation in

Table 1 The genes related to cuticle biosynthesis in RNA-seq assays

Gene symbol	Encoding proteins	FPKM (vector)	FPKM (AaMIXTA1-RNAi-3)	Function	Seq-id
LACS1	Long-chain-fatty-acid--CoA ligase 1	82.891	86.783	W/C	c101300_g1
LACS2	Long-chain-fatty-acid--CoA ligase 2	19.5	32.694	W/C	c105415_g1
CER6-like	3-ketoacyl-CoA synthase 6-like	16.311	6.253	W	c90325_g1
CER6	3-ketoacyl-CoA synthase 6	4.793	2.493	W	c111308_g1
KCR1	Beta-ketoacyl reductase 1	146.745	126.897	W	c82838_g1
PAS2	Protein-tyrosine phosphatase-like	16.24	4.062	W	c88021_g1
CER10	3-oxo-5-alpha-steroid 4-dehydrogenase	70.25	73.291	W	c96468_g1
CER26	ECERIFERUM 26	6.993	3.137	W	c103318_g1
CER4	ECERIFERUM 4	32.239	19.102	W	c104996_g1
GPAT6	Glycerol-3-phosphate acyltransferase 6	131.146	138.288	C	c100139_g2
GPAT3	Glycerol-3-phosphate acyltransferase 3	32.524	25.597	C	c97199_g1
WSD1	*O*-acyltransferase	20.48	10.265	C	c93888_g2
CER1	Fatty acid hydroxylase 1	143.413	75.865	W	c97459_g1
CER3(WAX2)	Fatty acid hydroxylase 3	67.747	48.539	W	c94941_g1
ABCG11	ABC transporter G family member 11	59.524	67.118	W/C	c105371_g1
ABCG12	ABC transporter G family member 12	32.337	23.375	W	c104894_g1
ABCG32	ABC transporter G family member 32	32.417	35.489	C	c105323_g2
CD1(GDSL)	GDSL esterase	80.797	48.378	C	c95905_g1
CER9	ECERIFERUM 9	30.208	18.378	W	c104237_g1
CER7	ECERIFERUM 7	31.205	21.907	W	c108324_g1
CYP77A1	CYP77A subfamily of cytochrome P450	67.337	54.079	C	c105431_g1
CYP77A2	CYP77A subfamily of cytochrome P450	33.165	53.284	C	c104761_g1
CYP77A3	CYP77A subfamily of cytochrome P450	146.281	128.998	C	c44205_g1
HTH(ACE)	Glucose-methanol-choline (GMC) oxidoreductase	91.647	64.293	C	c98322_g1
CYP86A4	CYP86A subfamily of cytochrome P450	39.045	37.45	W/C	c106320_g2
CYP86A2	CYP86A subfamily of cytochrome P450	1.764	0.171	W/C	c71497_g1
CYP86A1	CYP86A subfamily of cytochrome P450	140.161	13.12	W/C	c99499_g1
CYP86B1	CYP86A subfamily of cytochrome P450	7.456	2.674	W/C	c98118_g1
CYP86A8	CYP86A subfamily of cytochrome P450	68.246	69.551	W/C	c106320_g1
KCS1	3-ketoacyl-CoA synthase1	62.01	54.33	W	c98267_g1
KCS5	3-ketoacyl-CoA synthase5	49.405	21.656	W	c88550_g1
KCS12	3-ketoacyl-CoA synthase12	1.514	4.363	W	c74141_g1
KCS21	3-ketoacyl-CoA synthase21	31.686	27.406	W	c96132_g1
KCS4	3-ketoacyl-CoA synthase4	115.806	75.624	W	c91728_g1
KCS11	3-ketoacyl-CoA synthase11	61.137	49.916	W	c97779_g2
KCS10(FDH)	3-ketoacyl-CoA synthase10	453.623	380.108	W/C	c106841_g1
KCS19	3-ketoacyl-CoA synthase19	0.383	0.352	W	c89768_g1

W, putative genes involved in wax biosynthesis; C, putative genes involved in cutin biosynthesis; W/C, putative genes involved in wax and cutin biosynthesis; FPKM, fragments per kb of exon model per million mapped reads.

the nectar guides in *Mimulus lewisii* flowers (Yuan *et al.*, 2013). These researches showed that MIXTA and MIXTA-like transcription factors were involved in trichome formation. In the present study, we identified a MIXTA type transcription factor, AaMIXTA1, by bioinformatics analysis (Figs 1a–c, S2). Overexpression and repression of *AaMIXTA1* resulted in an increase and decrease in the number of glandular secretory trichomes (GSTs) and T-shaped nonsecretory trichomes (TSTs) in transgenic *Artemisia annua* plants compared to that of controls, respectively (Figs 3a–d, S3). The ethylene response factor-associated amphiphilic repression (EAR) motif chimeric repressor can influence the ability of protein–protein interactions to repress the expression of downstream genes by means of chromatin modification (Ohta *et al.*, 2001). Therefore, we fused EAR motif to the C-terminal region of *AaMIXTA1* and generated *AaMIXTA1-EAR* lines. The repression of AaMIXTA1 significantly reduced the density of GST and TST (Figs 3d,g, S3). *35S: MYB106-SRDX* Arabidopsis plants had trichomes that appeared to be immature and with abnormal branching (Oshima *et al.*, 2013). However, in our study, GST and TST in *AaMIXTA1-EAR* lines had a normal morphological structure (Fig. 4c,f,i). Phylogenetic analysis suggested that the protein sequence of AaMIXTA1 was much more similar to that of AmMYBML3 than AtMYB16 and AtMYB106 (Fig. 1b). These differences suggest that the molecular mechanism for formation of multicellular trichomes in *A. annua* may be very distinct from the one involved in formation of unicellular trichomes in Arabidopsis. Interestingly, Jindal *et al.* (2015) cloned a MIXTA homolog, AaMIXTA-like1, from *A. annua* and used a transient assay to show that its promoter was able to direct expression of a reporter in both GST and TSTs, but no functional analysis of the gene was undertaken.

Previous research has shown that artemisinin biosynthesis occurs exclusively in the glandular trichomes of *A. annua* (Olofsson *et al.*, 2011). Glandular trichomes are small multicellular protrusions from the epidermis on the surface of leaves and other

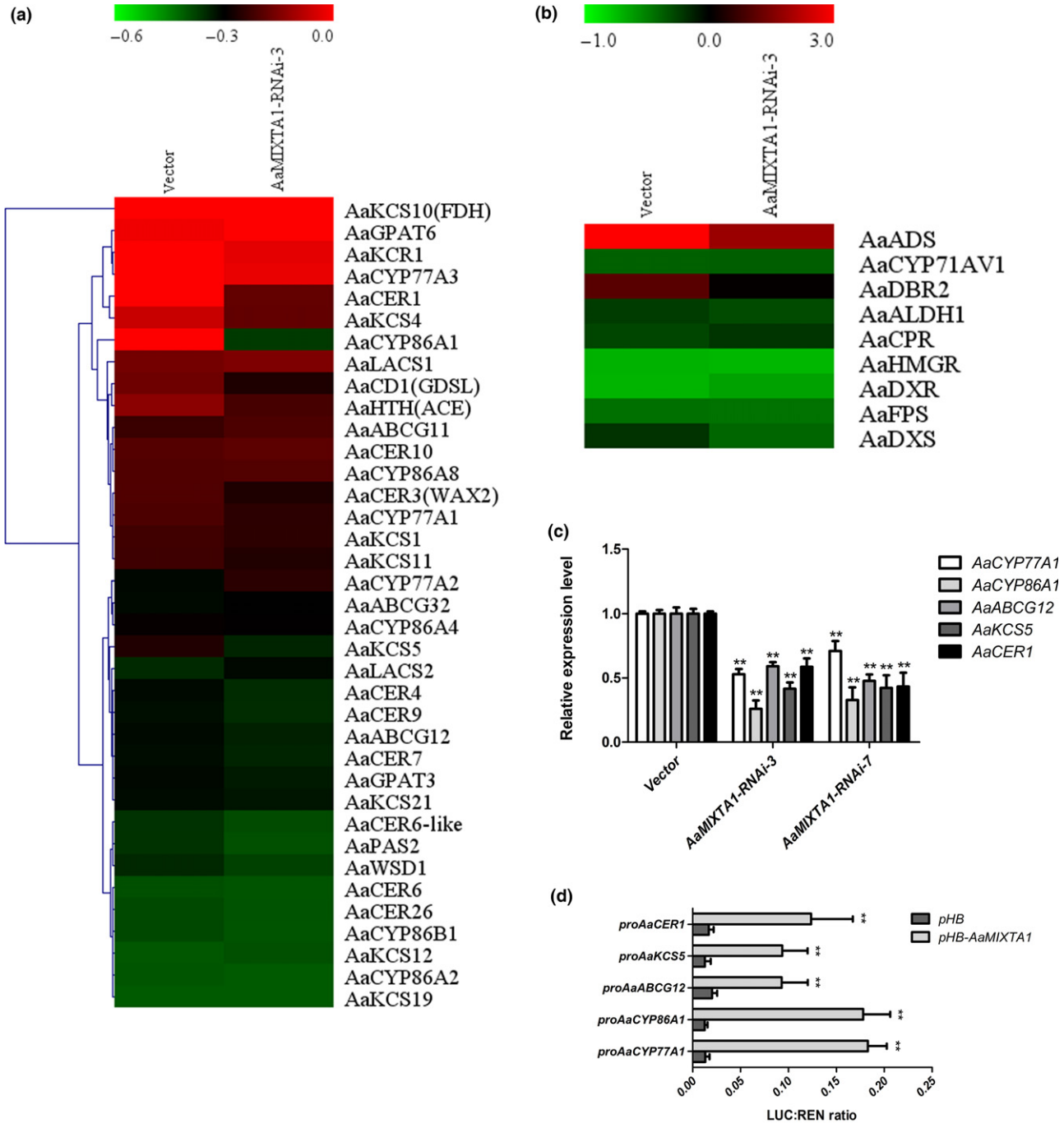

Fig. 6 AaMIXTA1 regulates the cuticle biosynthesis in *Artemisia annua*. (a, b) Hierarchical clustering analysis of genes involved in (a) cuticle biosynthesis and (b) artemisinin biosynthesis in empty vector (pHELLSGATE12) and *AaMIXTA1-RNAi* transgenic *A. annua* line. Rows represent differentially expressed (a) cuticle biosynthesis genes and (b) artemisinin biosynthesis genes, columns represent group comparison. Green and red boxes represent lower and higher gene expression levels, respectively. Color saturation reflects magnitude of logarithmic fold change (log_2FC) expression ratio for each absolute value. Each gene in the vertical axis is clustered by MeV hierarchical clustering (HCL) using Euclidean distance. Asterisks indicate repression of genes transcript levels involved in (a) cuticle biosynthesis and (b) artemisinin biosynthesis. (c) Quantitative real-time polymerase chain reaction analysis of genes involved in the cuticle biosynthesis in empty vector (pHELLSGATE12) and *AaMIXTA1-RNAi* transgenic *A. annua* lines. β-*Actin* is used as internal control. Three technical replicates were used for each biological repeat. Three biological repeats are measured for each sample. Data are given as means ± SD ($n = 3$). (d) Transient dual-luciferase (Dual-LUC) assay shows that AaMIXTA1 activates the expression of *AaKCS5*, *AaCER1*, *AaCYP77A1*, *AaCYP86A1* and *AaABCG12* in *Nicotiana benthamiana* leaves. The *proAaKCS5*, *proAaCER1*, *proAaCYP77A1*, *proAaCYP86A1* and *proAaABCG12* are fused to the LUC reporter to get the reporter construct. *35S: AaMIXTA1* is used as effector. Cauliflower mosaic virus (CaMV) 35S promoter promoter driven Renilla luciferase is used as the internal reference. Data are given as means ± SD ($n = 3$). Double asterisks indicate significant differences between transgenic plant and the control by Student's *t*-test. **, $P < 0.01$.

organs of *A. annua* (Olsson *et al.*, 2009). Increasing GST density could therefore be an effective approach to improve the artemisinin content. The previously characterized homeodomain regulator, AaHD1, also promotes glandular trichome initiation (Yan *et al.*, 2016) although the mechanism by which it regulates development of those trichomes has not yet been fully explored. In another recent study, overexpression of *AaMYB1* was used to increase artemisinin content and like AaMIXTA1 this was through increasing the density of GSTs (Matias-Hernandez *et al.*, 2017). AaMYB1 is related more to AtMYB61 and AtMYB50 than to any of the MIXTA-like factors, so it may function through a different mechanism to AaMIXTA1.

In Arabidopsis, the expression of *WIN1/SHN1*, encoding an AP2/ERF transcription factor, was regulated by MIXTA-like MYBs (Oshima *et al.*, 2013). The AP2 factor TRICHOME AND ARTEMISININ REGULATOR 1 (TAR1) has been reported to regulate trichome morphology in *A. annua* (Tan *et al.*, 2015). However, AaMIXTA1 did not appear to regulate TAR1 in *A. annua* (Fig. S5a,b). TAR1 affects trichome morphology rather than the density of the trichomes so is well downstream from AaMIXTA1. It would thus be interesting to investigate AaMIXTA1's regulation on the expression of AP2 transcription factors. SlMIXTA-like gene products possibly cooperating with homeodomain leucine zipper IV transcription factors could positively regulate both cuticle biosynthesis and epidermal cell formation in tomato (Lashbrooke *et al.*, 2015). In addition, the CUTIN DEFICIENT2 mutation *cd2* altered both trichome formation and cuticle biosynthesis in tomato (Nadakuduti *et al.*, 2012). The relationships between different MIXTA and HDZip IV transcription factors in regulating GST development in *A. annua* will need to be studied in greater detail in future.

Plant species such as *A. thaliana* only contain one type of trichome that is nonglandular, whereas other species such as tobacco have several different types of multicellular glandular trichomes. *Artemisia annua*, having one type of glandular and one type of nonglandular trichome, is emerging as a 'classical' model system for studying the formation mechanism of plant trichomes. It is, thus, worthwhile conducting further studies of trichome development in *A. annua* in the future.

AaMIXTA1 positively regulates cuticle deposition in *A. annua* leaves

The cuticle is the first physical and chemical barrier between a plant and its environment (Pollard *et al.*, 2008). GST density on the mature leaves in *A. annua* is predetermined at a primordial stage of leaf development (Duke & Paul, 1993; Davies *et al.*, 2009). The cuticle covers the subcuticular space of GSTs (Olsson *et al.*, 2009). Cuticle is secreted from epidermal cells to the outside of cell walls for attracting pollinators, protecting plants from biotic and abiotic stresses, and controlling plant morphology (Oshima *et al.*, 2013). The evolution of land plants certainly required the formation of the cuticular layer (Pollard *et al.*, 2008; Koch & Barthlott, 2009; Yeats *et al.*, 2012). Previous research shows that some MYB transcription factors regulate cuticle development in plants. In Arabidopsis, MYB106 regulates trichome branch formation by inducing the formation of cutin and epicuticular waxes (Oshima *et al.*, 2013). MYB41 controls cell expansion and cuticle deposition in response to abiotic stress (Cominelli *et al.*, 2008). MYB30 and MYB96 are involved in the biosynthesis of very-long-chain fatty acids (VLCFAs; Raffaele *et al.*, 2008; Seo *et al.*, 2011). Besides, two ABCG half-transporters, ABCG11/WBC11 and ABCG12/CER5, are implicated in lipid export from epidermis to cuticle (Pighin *et al.*, 2004; Bird *et al.*, 2007), with *abcg11* mutants displaying decreased cutin and wax contents (Bird *et al.*, 2007). The ABCG12/CER5 transporter is required for wax export, but not for cutin (Pighin *et al.*, 2004). GC-MS analyses of AaMIXTA1 overexpressing and RNAi lines provide strong evidence that this transcription factor modulates cuticle biosynthesis in *A. annua* (Fig. 5a–d). The expression of genes involved in cuticle biosynthesis was also detected by RNA-seq analysis (Fig. 6a). Repression of *AaMIXTA1* transcripts significantly reduced the expression of genes related to cuticle biosynthesis, including *AaCER1*, *AaKCS4*, *AaCYP86A1*, *AaCD1*, *AaHTH*, *AaCER3*, *AaCYP77A1*, *AaKCS11*, *AaKCS5*, *AaCER4*, *AaCER9*, *AaCER7*, *AaCER6*, *AaCER6-like*, *AaWSD1* and *ABCG12* (Fig. 6a). In plants, VLCFAs and their derivatives are constituents of the cuticular waxes (Jenks *et al.*, 1994; Samuels *et al.*, 2008). VLCFA derivatives form protective barriers between plants and the environment. In Arabidopsis, *KCS5*, encoding a 3-ketoacyl-CoA synthase, is involved in the biosynthesis of VLCFA (Todd *et al.*, 1999; Lee *et al.*, 2009). Overexpression of CER1 increased VLCFA biosynthesis and impaired leaf epidermal cell division and expansion (Bourdenx *et al.*, 2011). CYP77A1 and CYP86A1 are required for the polymerized cutin biosynthesis. Dual-LUC effector reporter assays showed that AaMIXTA1 activated the expression of *AaKCS5*, *AaCER1*, *AaCYP77A1*, *AaCYP86A1* and *AaABCG12* (Fig. 6d). Recent studies demonstrate that cuticle biosynthesis is closely linked to trichome initiation. TAR1 is a critical regulator involved in trichome differentiation and cuticle formation (Tan *et al.*, 2015). Overexpression of *AtCFL1* in whole *A. thaliana* plants resulted in misshapen and flattened trichomes in leaves, possibly related to a cuticle accumulation defect compared those of the wild-type (Wu *et al.*, 2011). GSTs and TSTs in *A. annua* are multicellular structures, so the mechanism involved in GST and TST formation in *A. annua* might be more complex than that of the unicellular trichomes in Arabidopsis. Our results, together with recent findings, suggest that AaMIXTA1 might upregulate the trichome initiation and affect the cuticle biosynthesis.

Overexpression of *AaMIXTA1* improves the content of artemisinin in *A. annua*

Artemisinin isolated from the medicinal plant *A. annua* is the most effective compound for the treatment of malaria (Ridley, 2003; Tu, 2011). To increase the artemisinin content, great efforts have been made to explore the transcriptional regulation on artemisinin biosynthesis. In recent years synthetic biology has opened up new options for the production of artemisinin in organisms other than *A. annua*. Model organisms such as tobacco and the moss *Phycomitrella patens* have been engineered to

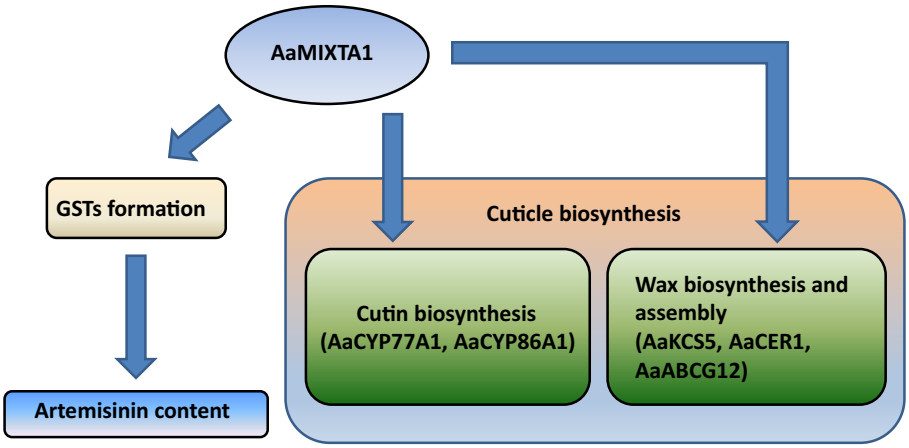

Fig. 7 The simplified model of AaMIXTA1 on the initiation of glandular secretory trichome (GST) and cuticle biosynthesis in *Artemisia annua*.

produce a range of secondary metabolites (Farhi *et al.*, 2011; Zhan *et al.*, 2014). Our approach was to increase artemisinin content by increasing the density of GSTs in *A. annua*. GSTs are regarded as the biofactory for secondary metabolite biosynthesis and storage. Although GSTs are essential for artemisinin biosynthesis, little is known about the mechanism of GST formation in *A. annua*. In the present study, overexpression of *AaMIXTA1* significantly increased GST density, resulting in an increase in artemisinin content in *A. annua* (Fig. 4j) without adversely affecting the structure of GSTs (Fig. 4d–f).

Conclusions

Glandular trichomes cover the surfaces of leaves, stems and flowers of many plants. GSTs have the capacity to secrete and store a large number of secondary metabolites. In this study, we identified an R2R3 MYB transcription factor, AaMIXTA1, which is involved in initiation of GSTs on leaves and also regulates cuticle biosynthesis in *A. annua* (Fig. 7). Our study provides a useful transcription factor and a strategy to improve artemisinin content in *A. annua* through increasing the number of GSTs where artemisinin is synthesized and stored.

Acknowledgements

This work was funded by China National High-Tech '863' Program (grant no. 2011AA100605), Shanghai Key Discipline Cultivation and Construction Project (Horticulture) and Shanghai Jiao Tong University Agri-Engineering Program. We thank the Instrumental Analysis Center of the Shanghai Jiao Tong University for assistance with GC-MS analysis.

Author contributions

P.S., X.F. and K.T. conceived and designed the entire research plans; P.S., X.F. and M.L. performed most of the experiments; Y.T., L.L., Q.S., Q.P., Z.L., T.Y., Y.M., M.C., P.L. and X.H. provided technical assistance to P.S. and X.F.; P.S. and K.T. wrote the manuscript; and X.S., L.L., X.F., Q.S., Q.P. and W.J. helped with the organization and editing.

References

Abdin MZ, Israr M, Rehman RU, Jain SK. 2003. Artemisinin, a novel antimalarial drug: biochemical and molecular approaches for enhanced production. *Planta Medica* **69**: 289–299.

Bernard A, Joubes J. 2013. *Arabidopsis* cuticular waxes: advances in synthesis, export and regulation. *Progress in Lipid Research* **52**: 110–129.

Bird D, Beisson F, Brigham A, Shin J, Greer S, Jetter R, Kunst L, Wu X, Yephremov A, Samuels L. 2007. Characterization of *Arabidopsis* ABCG11/WBC11, an ATP binding cassette (ABC) transporter that is required for cuticular lipid secretion. *Plant Journal* **52**: 485–498.

Bourdenx B, Bernard A, Domergue F, Pascal S, Leger A, Roby D, Pervent M, Vile D, Haslam RP, Napier JA *et al.* 2011. Overexpression of *Arabidopsis* ECERIFERUM1 promotes wax very-long-chain alkane biosynthesis and influences plant response to biotic and abiotic stresses. *Plant Physiology* **156**: 29–45.

Brockington SF, Alvarez-Fernandez R, Landis JB, Alcorn K, Walker RH, Thomas MM, Hileman LC, Glover BJ. 2013. Evolutionary analysis of the *MIXTA* gene family highlights potential targets for the study of cellular differentiation. *Molecular Biology and Evolution* **30**: 526–540.

Cheng Y, Cao L, Wang S, Li Y, Wang H, Zhou Y. 2014. Analyses of plant leaf cell size, density and number, as well as trichome number using cell counter plugin. *Bio-Protocol* **4**: e1165.

Chuartzman SG, Nevo R, Shimoni E, Charuvi D, Kiss V, Ohad I, Brumfeld V, Reich Z. 2008. Thylakoid membrane remodeling during state transitions in *Arabidopsis*. *Plant Cell* **20**: 1029–1039.

Cominelli E, Sala T, Calvi D, Gusmaroli G, Tonelli C. 2008. Over-expression of the *Arabidopsis AtMYB41* gene alters cell expansion and leaf surface permeability. *Plant Journal* **53**: 53–64.

Davies MJ, Atkinson CJ, Burns C, Woolley JG, Hipps NA, Arroo RR, Dungey N, Robinson T, Brown P, Flockart I *et al.* 2009. Enhancement of artemisinin concentration and yield in response to optimization of nitrogen and potassium supply to *Artemisia annua*. *Annals of Botany* **104**: 315–323.

Dubos C, Stracke R, Grotewold E, Weisshaar B, Martin C, Lepiniec L. 2010. MYB transcription factors in *Arabidopsis*. *Trends in Plant Science* **15**: 573–581.

Duke SO, Paul RN. 1993. Development and fine structure of the glandular trichomes of *Artemisia annua* L. *International Journal of Plant Sciences* **154**: 107–118.

Efferth T. 2006. Molecularpharmacology and pharmacogenomics of artemisinin and its derivatives in cancer cells. *Current Drug Targets* **7**: 407–421.

Farhi M, Marhevka E, Ben-Ari J, Algamas-Dimantov A, Liang Z, Zeevi V, Edelbaum O, Spitzer-Rimon B, Abeliovich H, Schwartz B *et al.* 2011. Generation of the potent anti-malarial drug artemisinin in tobacco. *Nature Biotechnology* **29**: 1072–1074.

Feller A, Machemer K, Braun EL, Grotewold E. 2011. Evolutionary and comparative analysis of MYB and bHLH plant transcription factors. *Plant Journal* **66**: 94–116.

Franke R, Briesen I, Wojciechowski T, Faust A, Yephremov A, Nawrath C, Schreiber L. 2005. Apoplastic polyesters in *Arabidopsis* surface tissues – a typical suberin and a particular cutin. *Phytochemistry* **66**: 2643–2658.

Glover BJ, Perezrodriguez M, Martin CM. 1998. Development of several epidermal cell types can be specified by the same MYB-related plant transcription factor. *Development* **125**: 3497–3508.

Go YS, Kim H, Kim HJ, Suh MC. 2014. *Arabidopsis* cuticular wax biosynthesis is negatively regulated by the DEWAX gene encoding an AP2/ERF-type transcription factor. *Plant Cell* **26**: 1666–1680.

Graham IA, Besser K, Blumer S, Branigan CA, Czechowski T, Elias L, Guterman I, Harvey D, Isaac PG, Khan AM. 2010. The genetic map of *Artemisia annua* L. identifies loci affecting yield of the antimalarial drug artemisinin. *Science* **327**: 328–331.

Hellens RP, Allan AC, Friel EN, Bolitho K, Grafton K, Templeton MD, Karunairetnam S, Gleave AP, Laing WA. 2005. Transient expression vectors for functional genomics, quantification of promoter activity and RNA silencing in plants. *Plant Methods* **1**: 13.

Jakoby MJ, Falkenhan D, Mader MT, Brininstool G, Wischnitzki E, Platz N, Hudson A, Hulskamp M, Larkin J, Schnittger A. 2008. Transcriptional profiling of mature *Arabidopsis* trichomes reveals that *NOECK* encodes the MIXTA-like transcriptional regulator MYB106. *Plant Physiology* **148**: 1583–1602.

Jefferson RA, Kavanagh TA, Bevan MW. 1987. GUS fusions: beta-glucuronidase as a sensitive and versatile gene fusion marker in higher plants. *The EMBO Journal* **6**: 3901–3907.

Jenks MA, Joly RJ, Peters PJ, Rich PJ, Axtell JD, Ashworth EN. 1994. Chemically induced cuticle mutation affecting epidermal conductance to water vapor and disease susceptibility in *Sorghum bicolor* (L.) Moench. *Plant Physiology* **105**: 1239–1245.

Jindal S, Longchar B, Singh A, Gupta V. 2015. Promoters of *AaGL2* and *AaMIXTA-Like1* genes of *Artemisia annua* direct reporter gene expression in glandular and non-glandular trichomes. *Plant Signaling and Behavior* **10**: e1087629.

Jungblut P, Schaible U, Mollenkopf HJ, Zimny-Arndt U, Raupach B, Mattow J, Halada P, Lamer S, Hagens K, Kaufmann S. 1999. Comparative proteome analysis of *Mycobacterium tuberculosis* and *Mycobacterium bovis* BCG strains: towards functional genomics of microbial pathogens. *Molecular Microbiology* **33**: 1103–1117.

Kannangara R, Branigan C, Liu Y, Penfield T, Rao V, Mouille G, Hofte H, Pauly M, Riechmann JL, Broun P. 2007. The transcription factor WIN1/SHN1 regulates cutin biosynthesis in *Arabidopsis thaliana*. *Plant Cell* **19**: 1278–1294.

Karimi M, Depicker A, Hilson P. 2007. Recombinational cloning with plant gateway vectors. *Plant Physiology* **145**: 1144–1154.

Khosla A, Paper JM, Boehler AP, Bradley AM, Neumann TR, Schrick K. 2014. HD-Zip proteins GL2 and HDG11 have redundant functions in *Arabidopsis* trichomes, and GL2 activates a positive feedback loop via MYB23. *Plant Cell* **26**: 2184–2200.

Koch K, Barthlott W. 2009. Superhydrophobic and superhydrophilic plant surfaces: an inspiration for biomimetic materials. *Philosophical Transactions of the Royal Society A* **367**: 1487–1509.

Lashbrooke J, Adato A, Lotan O, Alkan N, Tsimbalist T, Rechav K, Fernandez-Moreno JP, Widemann E, Grausem B, Pinot F *et al.* 2015. The Tomato MIXTA-like transcription factor coordinates fruit epidermis conical cell development and cuticular lipid biosynthesis and assembly. *Plant Physiology* **169**: 2553–2571.

Lee S-B, Jung S-J, Go Y-S, Kim H-U, Kim J-K, Cho H-J, Park OK, Suh M-C. 2009. Two *Arabidopsis* 3-ketoacyl CoA synthase genes, *KCS20* and *KCS2/DAISY*, are functionally redundant in cuticular wax and root suberin biosynthesis, but differentially controlled by osmotic stress. *Plant Journal* **60**: 462–475.

Lee SB, Suh MC. 2015. Cuticular wax biosynthesis is up-regulated by the MYB94 transcription factor in *Arabidopsis*. *Plant and Cell Physiology* **56**: 48–60.

Liu H, Yu X, Li K, Klejnot J, Yang H, Lisiero D, Lin C. 2008. Photoexcited CRY2 interacts with CIB1 to regulate transcription and floral initiation in *Arabidopsis*. *Science* **322**: 1535.

Livak KJ, Schmittgen TD. 2001. Analysis of relative gene expression data using real-time quantitative PCR and the $2^{-\Delta\Delta C}{}_{T}$ method. *Methods* **25**: 402–408.

Machado A, Wu Y, Yang Y, Llewellyn DJ, Dennis ES. 2009. The MYB transcription factor GhMYB25 regulates early fibre and trichome development. *Plant Journal* **59**: 52–62.

Marco J, Barbera O. 1990. Natural products from the genus *Artemisia* L. *Studies in Natural Products Chemistry* **7**: 201–264.

Martin C, Bhatt K, Baumann K, Jin H, Zachgo S, Roberts K, Schwarz-Sommer Z, Glover B, Perez-Rodrigues M. 2002. The mechanics of cell fate determination in petals. *Philosophical Transactions of the Royal Society B* **357**: 809–813.

Martin C, Paz-Ares J. 1997. MYB transcription factors in plants. *Trends in Genetics* **13**: 67–73.

Matas AJ, Yeats TH, Buda GJ, Zheng Y, Chatterjee S, Tohge T, Ponnala L, Adato A, Aharoni A, Stark R *et al.* 2011. Tissue- and cell-type specific transcriptome profiling of expanding tomato fruit provides insights into metabolic and regulatory specialization and cuticle formation. *Plant Cell* **23**: 3893–3910.

Matias-Hernandez L, Jiang W, Yang K, Tang K, Brodelius PE, Pelaz S. 2017. AaMYB1 and its orthologue AtMYB61 affect terpene metabolism and trichome development in *Artemisia annua* and *Arabidopsis thaliana*. *Plant Journal* **90**: 520–534.

Mauricio R, Rausher MD. 1997. Experimental manipulation of putative selective agents provides evidence for the role of natural enemies in the evolution of plant defense. *Evolution* **51**: 1435–1444.

Mutabingwa TK. 2005. Artemisinin-based combination therapies (ACTs): best hope for malaria treatment but inaccessible to the needy! *Acta Tropica* **95**: 305–315.

Nadakuduti SS, Pollard M, Kosma DK, Allen C Jr, Ohlrogge JB, Barry CS. 2012. Pleiotropic phenotypes of the *sticky peel* mutant provide new insight into the role of *CUTIN DEFICIENT2* in epidermal cell function in tomato. *Plant Physiology* **159**: 945–960.

Noda K-i, Glover BJ, Linstead P, Martin C. 1994. Flower colour intensity depends on specialized cell shape controlled by a *Myb*-related transcription factor. *Nature* **369**: 661–664.

Ohta M, Matsui K, Hiratsu K, Shinshi H, Ohme-Takagi M. 2001. Repression domains of class II ERF transcriptional repressors share an essential motif for active repression. *Plant Cell* **13**: 1959–1968.

Olofsson L, Engström A, Lundgren A, Brodelius PE. 2011. Relative expression of genes of terpene metabolism in different tissues of *Artemisia annua* L. *BMC Plant Biology* **11**: 45.

Olofsson L, Lundgren A, Brodelius PE. 2012. Trichome isolation with and without fixation using laser microdissection and pressure catapulting followed by RNA amplification: expression of genes of terpene metabolism in apical and sub-apical trichome cells of *Artemisia annua* L. *Plant Science* **183**: 9–13.

Olsson ME, Olofsson LM, Lindahl AL, Lundgren A, Brodelius M, Brodelius PE. 2009. Localization of enzymes of artemisinin biosynthesis to the apical cells of glandular secretory trichomes of *Artemisia annua* L. *Phytochemistry* **70**: 1123–1128.

Oshima Y, Shikata M, Koyama T, Ohtsubo N, Mitsuda N, Ohme-Takagi M. 2013. MIXTA-Like transcription factors and WAX INDUCER1/SHINE1 coordinately regulate cuticle development in *Arabidopsis* and *Torenia fournieri*. *Plant Cell* **25**: 1609–1624.

Panikashvili D, Savaldi-Goldstein S, Mandel T, Yifhar T, Franke RB, Hofer R, Schreiber L, Chory J, Aharoni A. 2007. The *Arabidopsis* DESPERADO/AtWBC11 transporter is required for cutin and wax secretion. *Plant Physiology* **145**: 1345–1360.

Perez-Rodriguez M, Jaffe FW, Butelli E, Glover BJ, Martin C. 2005. Development of three different cell types is associated with the activity of a specific MYB transcription factor in the ventral petal of *Antirrhinum majus* flowers. *Development* **132**: 359–370.

Pighin JA, Zheng H, Balakshin LJ, Goodman IP, Western TL, Jetter R, Kunst L, Samuels AL. 2004. Plant cuticular lipid export requires an ABC transporter. *Science* **306**: 702–704.

Pollard M, Beisson F, Li Y, Ohlrogge JB. 2008. Building lipid barriers: biosynthesis of cutin and suberin. *Trends in Plant Science* **13**: 236–246.

Raffaele S, Vailleau F, Leger A, Joubes J, Miersch O, Huard C, Blee E, Mongrand S, Domergue F, Roby D. 2008. A MYB transcription factor regulates very-long-chain fatty acid biosynthesis for activation of the hypersensitive cell death response in *Arabidopsis*. *Plant Cell* **20**: 752–767.

Ridley RG. 2003. Malaria: to kill a parasite. *Nature* **424**: 887–889.

Romero MR, Serrano MA, Vallejo M, Efferth T, Alvarez M, Marin J. 2006. Antiviral effect of artemisinin from *Artemisia annua* against a model member of the *Flaviviridae* family, the bovine viral diarrhoea virus (BVDV). *Planta Medica* **72**: 1169–1174.

Samuels L, Kunst L, Jetter R. 2008. Sealing plant surfaces: cuticular wax formation by epidermal cells. *Annual Review of Plant Biology* **59**: 683–707.

Schilmiller AL, Last RL, Pichersky E. 2008. Harnessing plant trichome biochemistry for the production of useful compounds. *Plant Journal* **54**: 702–711.

Seo PJ, Lee SB, Suh MC, Park MJ, Go YS, Park CM. 2011. The MYB96 transcription factor regulates cuticular wax biosynthesis under drought conditions in *Arabidopsis*. *Plant Cell* **23**: 1138–1152.

Serna L, Martin C. 2006. Trichomes: different regulatory networks lead to convergent structures. *Trends in Plant Science* **11**: 274–280.

Shen Q, Lu X, Yan T, Fu X, Lv Z, Zhang F, Pan Q, Wang G, Sun X, Tang K. 2016. The jasmonate-responsive AaMYC2 transcription factor positively regulates artemisinin biosynthesis in *Artemisia annua*. *New Phytologist* **210**: 1269–1281.

Slone JH, Kelsey RG. 1985. Isolation and purification of glandular secretory cells from *Artemisia tridentata* (ssp. *vaseyana*) by Percoll density gradient centrifugation. *American Journal of Botany* **72**: 1445–1451.

Sparkes IA, Runions J, Kearns A, Hawes C. 2006. Rapid, transient expression of fluorescent fusion proteins in tobacco plants and generation of stably transformed plants. *Nature Protocols* **1**: 2019–2025.

Stracke R, Ishihara H, Huep G, Barsch A, Mehrtens F, Niehaus K, Weisshaar B. 2007. Differential regulation of closely related R2R3-MYB transcription factors controls flavonol accumulation in different parts of the *Arabidopsis thaliana* seedling. *Plant Journal* **50**: 660–677.

Stracke R, Werber M, Weisshaar B. 2001. The R2R3-MYB gene family in *Arabidopsis thaliana*. *Current Opinion in Plant Biology* **4**: 447–456.

Suo B, Seifert S, Kirik V. 2013. *Arabidopsis GLASSY HAIR* genes promote trichome papillae development. *Journal of Experimental Botany* **64**: 4981–4991.

Tamura K, Peterson D, Peterson N, Stecher G, Nei M, Kumar S. 2011. MEGA5: molecular evolutionary genetics analysis using maximum likelihood, evolutionary distance, and maximum parsimony methods. *Molecular Biology and Evolution* **28**: 2731–2739.

Tan H, Xiao L, Gao S, Li Q, Chen J, Xiao Y, Ji Q, Chen R, Chen W, Zhang L. 2015. *TRICHOME AND ARTEMISININ REGULATOR 1* is required for trichome development and artemisinin biosynthesis in *Artemisia annua*. *Molecular Plant* **8**: 1396–1411.

Tang K, Shen Q, Yan T, Fu X. 2014. Transgenic approach to increase artemisinin content in *Artemisia annua* L. *Plant Cell Reports* **33**: 605–615.

Todd J, Post-Beittenmiller D, Jaworski Jan G. 1999. *KCS1* encodes a fatty acid elongase 3-ketoacyl-CoA synthase affecting wax biosynthesis in *Arabidopsis thaliana*. *Plant Journal* **17**: 119–130.

Tu Y. 2011. The discovery of artemisinin (qinghaosu) and gifts from Chinese medicine. *Nature Medicine* **17**: 1217–1220.

Utzinger J, Xiao S-H, Tanner M, Keiser J. 2007. Artemisinins for schistosomiasis and beyond. *Current Opinion in Investigational Drugs* **8**: 105–116.

Voinnet O, Rivas S, Mestre P, Baulcombe D. 2003. An enhanced transient expression system in plants based on suppression of gene silencing by the p19 protein of tomato bushy stunt virus. *Plant Journal* **33**: 949–956.

Walford SA, Wu Y, Llewellyn DJ, Dennis ES. 2011. GhMYB25-like: a key factor in early cotton fibre development. *Plant Journal* **65**: 785–797.

Wang H, Han J, Kanagarajan S, Lundgren A, Brodelius PE. 2013. Trichome-specific expression of the amorpha-4,11-diene 12-hydroxylase (*cyp71av1*) gene, encoding a key enzyme of artemisinin biosynthesis in *Artemisia annua*, as reported by a promoter-GUS fusion. *Plant Molecular Biology* **81**: 119–138.

Weathers PJ, Arsenault PR, Covello PS, McMickle A, Teoh KH, Reed DW. 2011. Artemisinin production in *Artemisia annua*: studies *in planta* and results of a novel delivery method for treating malaria and other neglected diseases. *Phytochemistry Reviews* **10**: 173–183.

Wester K, Digiuni S, Geier F, Timmer J, Fleck C, Hulskamp M. 2009. Functional diversity of R3 single-repeat genes in trichome development. *Development* **136**: 1487–1496.

Wu R, Li S, He S, Wassmann F, Yu C, Qin G, Schreiber L, Qu LJ, Gu H. 2011. CFL1, a WW domain protein, regulates cuticle development by modulating the function of HDG1, a class IV homeodomain transcription factor, in rice and *Arabidopsis*. *Plant Cell* **23**: 3392–3411.

Yan T, Chen M, Shen Q, Li L, Fu X, Pan Q, Tang Y, Shi P, Lv Z, Jiang W *et al.* 2016. HOMEODOMAIN PROTEIN 1 is required for jasmonate-mediated glandular trichome initiation in *Artemisia annua*. *New Phytologist* **213**: 1145–1155.

Yeats TH, Martin LB, Viart HM, Isaacson T, He Y, Zhao L, Matas AJ, Buda GJ, Domozych DS, Clausen MH *et al.* 2012. The identification of cutin synthase: formation of the plant polyester cutin. *Nature Chemical Biology* **8**: 609–611.

Yuan Y-W, Sagawa JM, Di Stilio VS, Bradshaw HD. 2013. Bulk segregant analysis of an induced floral mutant identifies a MIXTA-Like R2R3 MYB controlling nectar guide formation in *Mimulus lewisii*. *Genetics* **194**: 523–528.

Zhan X, Zhang Y-H, Chen D-F, Simonsen HT. 2014. Metabolic engineering of the moss *Physcomitrella patens* to produce the sesquiterpenoids patchoulol and α/β-santalene. *Frontiers in Plant Science* **5**: 636.

Zhang F, Fu X, Lv Z, Lu X, Shen Q, Zhang L, Zhu M, Wang G, Sun X, Liao Z *et al.* 2015. A basic leucine zipper transcription factor, AabZIP1, connects abscisic acid signaling with artemisinin biosynthesis in *Artemisia annua*. *Molecular Plant* **8**: 163–175.

Zhang L, Jing F, Li F, Li M, Wang Y, Wang G, Sun X, Tang K. 2009. Development of transgenic *Artemisia annua* (Chinese wormwood) plants with an enhanced content of artemisinin, an effective anti-malarial drug, by hairpin-RNA-mediated gene silencing. *Biotechnology and Applied Biochemistry* **52**: 199–207.

Zheng H, Rowland O, Kunst L. 2005. Disruptions of the *Arabidopsis* Enoyl-CoA reductase gene reveal an essential role for very-long-chain fatty acid synthesis in cell expansion during plant morphogenesis. *Plant Cell* **17**: 1467–1481.

Supporting Information

Additional Supporting Information may be found online in the Supporting Information tab for this article:

Fig. S1 Artemisinin biosynthesis in *Artemisia annua*.

Fig. S2 Phylogenetic analysis between nine candidate MYB transcription factors in *Artemisia annua* and partial *Arabidopsis* MYB transcription factors.

Fig. S3 *AaMIXTA1* regulates T-shaped nonsecretory trichome initiation in *Artemisia annua*.

Fig. S4 The expression of genes involved in artemisinin biosynthesis in empty vector (pHELLSGATE12) and *AaMIXTA1-RNAi* transgenic plants.

Fig. S5 The expression of *TRICHOME AND ARTEMISININ REGULATOR 1* (*TAR1*).

Table S1 Primers used in this study

Table S2 Primers used for quantitative RT-PCR analysis in this study

Table S3 Statistical data of RNA-seq data

Table S4 Genes with differential expression between empty vector (pHELLSGATE12) and *AaMIXTA1-RNAi* transgenic *Artemisia annua* plants

Please note: Wiley Blackwell are not responsible for the content or functionality of any Supporting Information supplied by the authors. Any queries (other than missing material) should be directed to the *New Phytologist* Central Office.